

Gamma-Tocotrienol Modulates Radiation-Induced MicroRNA Expression in Mouse Spleen

Sanchita P. Ghosh,^{a,1,2} Rupak Pathak,^{b,2} Parammeet Kumar,^{c,2} Shukla Biswas,^a Sharmistha Bhattacharyya,^d Vidya P. Kumar,^a Martin Hauer-Jensen^b and Roopa Biswas^{c,1}

^a Armed Forces Radiobiology Research Institute, Uniformed Services University of the Health Sciences Scientific Research Department, Armed Forces Radiobiology Research Institute, Uniformed Services University of the Health Sciences, Bethesda, Maryland; ^b Division of Radiation Health, University of Arkansas for Medical Sciences, Little Rock, Arkansas; ^c Anatomy, Physiology and Genetics, School of Medicine, Uniformed Services University of the Health Sciences, Bethesda, Maryland; and ^d Endocrinology Division, CSIR-Central Drug Research Institute, Lucknow 226024, India

Ghosh, S. P., Pathak, R., Kumar, P., Biswas, S., Bhattacharyya, S., Kumar, V. P., Hauer-Jensen, M. and Biswas, R. Gamma-Tocotrienol Modulates Radiation-Induced MicroRNA Expression in Mouse Spleen. *Radiat. Res.* **185**, 485–495 (2016).

Ionizing radiation causes depletion of hematopoietic cells and enhances the risk of developing secondary hematopoietic malignancies. Vitamin E analog gamma-tocotrienol (GT3), which has anticancer properties, promotes postirradiation hematopoietic cell recovery by enhancing spleen colony-forming capacity, and provides protection against radiation-induced lethality in mice. However, the underlying molecular mechanism involved in GT3-mediated postirradiation survival is not clearly understood. Recent studies have shown that natural dietary products including vitamin E provide a benefit to biological systems by modulating microRNA (miR) expression. In this study, we show that GT3 differentially modulates the miR footprint in the spleen of irradiated mice compared to controls at early times (day 1), as well as later times (day 4 and 15) after total-body irradiation. We observed that miR expression was altered in a dose- and time-dependent manner in GT3-pretreated spleen tissues from total-body irradiated mice. GT3 appeared to affect the expression of a number of radiation-modulated miRs known to be involved in hematopoiesis and lymphogenesis. Moreover, GT3 pretreatment also suppressed the upregulation of radiation-induced p53, suggesting the function of GT3 in the prevention of radiation-induced damage to the spleen. In addition, we have shown that GT3 significantly reduced serum levels of Flt3L, a biomarker of radiation-induced bone marrow aplasia. Further *in silico* analyses of the effect of GT3 implied the association of p38 MAPK, ERK and insulin

signaling pathways. Our study provides initial insight into the mechanism by which GT3 mediates protection of spleen after total-body irradiation. © 2016 by Radiation Research Society

INTRODUCTION

Normal tissue injury, particularly hematopoietic damage, is a major concern in radiotherapy due to its potential toxic side effects, thus limiting its cancer cure rate (1, 2). Nonclinical exposure to ionizing radiation (accidental or deliberate) results in multi-organ dysfunction syndrome (MODS), which can lead to acute radiation syndrome (ARS) and/or long-term health effects such as cancer or pulmonary fibrosis, depending on dose rate and total absorbed dose (3, 4). ARS includes hematopoietic syndrome manifested as peripheral blood pancytopenia, with depletion of bone marrow progenitor cells and damage to the hematopoietic organs including the spleen (5, 6). Moreover, exposure to ionizing radiation increases the risk of cancer development and progression (7). Therefore, the development of strategies to prevent radiation-induced damage is essential. There is an urgent need to develop radiation countermeasure drugs that can be administered prior to radiation therapy for cancer patients, and prior to exposure for first responders and military personnel during rescue operations. However, to date there is only one FDA-approved radiation countermeasure drug (Neupogen®) available. Our studies have demonstrated that a vitamin E analog, gamma tocotrienol (GT3), protected mice from lethal doses of radiation partially by preventing postirradiation pancytopenia (8), depletion of bone marrow progenitor cells (9) and reduction in colony-forming capacity of spleen (10). Other studies have reported potent anticancer activity of GT3 (11, 12). However, the molecular mechanism by which GT3 prevents spleen damage to protect the hematopoietic system and increase mouse survival remains elusive.

Editor's note. The online version of this article (DOI: 10.1667/RR14248.1) contains supplementary information that is available to all authorized users.

¹ Address for correspondence: Scientific Research Department, Armed Forces Radiobiology Research Institute, Uniformed Services University of the Health Sciences, 8901 Wisconsin Ave. Bethesda, MD 20889-5603; e-mail: sanchita.ghosh@usuhs.edu or roopa.biswas@usuhs.edu.

² These authors contributed equally to this work.

Vitamin E has been shown to exert beneficial effects by modulating microRNA (miR, miRNA) profiles in different tissues (13). MiRs are endogenous noncoding RNAs, about 19–22 nucleotides in length, identified as regulators of gene expression by inducing cleavage of their target mRNAs and/or repression of translation. An earlier study has shown that vitamin E deficiency results in differential miR expression in liver tissue of rats (13). A recent study has demonstrated that tocotrienol-rich fraction prevents cellular senescence by modulating the expression of senescence-activated miRs (14). Although the function of vitamin E in modulating miR expression is well established, the role of GT3 in modulating radiation-induced miR expression is not well defined.

Several studies have analyzed the effect of radiation on miR expression (15–18). Radiation has been shown to alter miR expression in peripheral blood and various tissues (15, 19). Plasma miRNA profile is highly predictive of different levels of radiation exposure and can serve as biomarkers to assess radiation dose after mass casualty scenarios (16, 20). Serum miR-150, a microRNA abundant in lymphocytes, exhibits a dose- and time-dependent decrease in expression after irradiation and has therefore been regarded as a sensitive biomarker for radiation-induced lymphocyte depletion and bone marrow damage (17). Ionizing radiation is known to induce cellular stress by generating free radicals, which in turn cause DNA damage. Damaged DNA modulates an array of miR expression in a p53-dependent and -independent manner, as evident in *in vitro* (17, 21–23) and *in vivo* (18, 24) studies. MiR-34a, which is a direct target of p53, was reported to show potent anti-proliferative effects. Moreover, miR-34a exhibits a time-dependent increase in serum and spleen in response to radiation and is a potential indicator of radiation-induced injury (25).

miRs regulate diverse cellular processes that may activate stress response signals, which in turn may affect radiation-induced injury in different animal tissues (26). Recent studies indicate that radiation upregulates miR-30b and miR-30c in human hematopoietic CD34⁺ cells, and miR-30c plays a critical role in cell damage through negative regulation of REDD1 (17). Moreover, our recent studies have also demonstrated the role of the radiation countermeasure delta-tocotrienol (DT3, a vitamin E isomer) in *in vitro* and *in vivo* regulation of miR-30 (27). We have shown that DT3 protected mouse and human CD34⁺ cells from radiation-induced apoptosis by inhibiting IL-1 β and miR-30 expression, resulting in increased survival of irradiated mice (27). Here we report the radiation-regulated miRs in spleen that may be involved in the radioprotection by GT3. We have identified dose- and time-dependent miRNA signatures in mouse spleen after total-body irradiation (TBI). Consequently, we also observed that GT3 modulates serum levels of Flt3L, a biomarker of radiation-induced bone marrow aplasia (28). An understanding of the molecular pathways associated with mechanisms by which GT3 protects against radiation-induced damage to the spleen

after whole-body exposure will lead to the development of novel therapeutics.

MATERIALS AND METHODS

Mice

Male CD2F1 mice (8–10 weeks old) were purchased from Harlan® Laboratories Inc. (Indianapolis, IN) and housed in an air-conditioned facility at the Armed Forces Radiobiology Research Institute (AFRRI; Bethesda, MD), which is accredited by the Association for Assessment and Accreditation of Laboratory Animal Care International (AAALAC). All mice were kept in rooms with a 12:12 h light/dark schedule at 21 \pm 2°C with 10–15 hourly cycles of fresh air and a relative humidity of 50 \pm 10%. Mice were held in quarantine for 2 weeks and were used after microbiology, serology and histopathology examination of representative samples ensured the absence of *Pseudomonas aeruginosa* and common murine diseases. Mice were provided with certified rodent rations (Harlan Teklad Rodent Diet no. 8604; Harlan Teklad, Madison, WI) and acidified water (with HCl, pH 2.5–3.0) *ad libitum*. All animal procedures were performed in accordance with a protocol approved by the Institutional Animal Care and Use Committee (IACUC) using the principles and procedures outlined in the National Research Council's *Guide for the Care and Use of Laboratory Animals*.

Drug Preparation and Administration

GT3 was formulated in 5% Tween® 80 (Yasoo Health Inc., Johnson City, TN) and a single subcutaneous (s.c.) injection was administered at a dose of 200 mg/kg (for an average weight of 25 g per mouse) in a volume of 0.1 ml. The vehicle was administered s.c. as an equivalent dose volume of 5% Tween 80 (0.1 ml) in saline.

Samples of drug formulation and vehicle were sent to Charles Rivers Laboratories (Charleston, SC) for endotoxin testing prior to initiation of the experiments. All samples yielded an endotoxin limit of less than 0.50 endotoxin units (EU), which is acceptable for drug testing in mice according to IACUC standards.

Irradiation

Mice were irradiated bilaterally in the AFRRI's 60-cobalt gamma irradiation facility in well ventilated plexiglass boxes (8 mice per box) at a dose rate of 0.6 Gy/min to total midline doses of 4 and 8 Gy, as described below. An alanine/ESR (electron spin resonance) dosimetry system (American Society for Testing and Material Standard E 1607) was used to measure dose rates (to water) in the cores of acrylic mouse phantoms. Phantoms were 3 inches long and 1 inch in diameter and were located in 50% of the compartments of the exposure rack. The ESR signals were measured with a calibration curve based on standard calibration dosimeters provided by the National Institute of Standard and Technology (NIST, Gaithersburg, MD). The accuracy of the calibration curve was verified by intercomparison with the National Physical Laboratory (NPL, Teddington, UK). The only corrections applied to the dose rates in phantoms were for the decay of the ⁶⁰Co source and for a small difference in mass energy-absorption coefficients for water and soft tissue. The radiation field was uniform within \pm 2%. After irradiation, mice were returned to their original cages with access to food and water *ad libitum* (8, 9). All irradiations were performed in the morning to minimize the diurnal effect.

Spleen Harvesting and Total RNA Extraction

Mice [n = 3 per group: nonirradiated vehicle (Veh 0 Gy); nonirradiated GT3 (GT3 0 Gy); Veh 4 Gy; GT3 4 Gy; Veh 8 Gy; and GT3 8 Gy] were sacrificed using CO₂ overdose followed by cervical dislocation, in accordance with IACUC approved protocol, on day 1, 4 and 15 postirradiation. Spleens were harvested at each time

point and immediately snap frozen in liquid nitrogen and stored at -80°C until use. Approximately 50 mg of the frozen tissue was homogenized by brief sonication in ice and total RNA were extracted using mirVana total RNA isolation kits (Life Technologies, Frederick, MD) following the manufacturer's protocol. RNA yield and quality was analyzed on a NanoDropTM spectrophotometer ND-1000 (Thermo Fisher Scientific Inc., Rockville, MD).

miRNA Microarray

Microarray hybridization and data analyses were performed by the commercial service provider, LC Sciences (www.lcsciences.com; Houston, TX) and miRBase v. 19.0 (http://www.mirbase.org/) was used to study the expression profiling of 1,265 unique mature mouse miRNAs using a μ Paraflo[®] microfluidic technology (29, 30). Briefly, the total RNA sample (1 μg) was 3' extended with a poly(A) tail using poly(A) polymerase. An oligonucleotide tag was then ligated to the poly(A) tail for later fluorescent dye staining and hybridization was performed overnight on a mirco paraflo microfluidic chip using a micro-circulation pump (Atactic Technologies Inc., Houston, TX) (29, 30). Each detection probe was chemically modified nucleotide coding segment complementary to target microRNA (from miRBase) and a spacer segment of polyethylene glycol to extend the coding segment away from the substrate. The detection probes were made using PGR (photogenerated reagent) chemistry by *in situ* synthesis and the hybridization melting temperatures were balanced by chemical modifications of the detection probes. For hybridization buffer, 100 μl 6 \times SSPE (0.90 M NaCl, 60 mM Na₂HPO₄, 6 mM EDTA, pH 6.8) containing 25% formamide was used at 34°C . After RNA hybridization, tag-conjugating Cy3 and Cy5 dyes were circulated through the microfluidic chip for dye staining and the fluorescence-hybridized images were collected using a laser scanner (GenePix[®] 4000B; Molecular Devices, Sunnyvale, CA) and digitized using Array-Pro image analysis software (Media Cybernetics, Rockville, MD).

miRNA Expression Analysis (qRT-PCR)

The miRNA expression data from the arrays were validated for a selected set of miRs by individual TaqMan[®] assays (Life Technologies) specific for the respective miRNAs. The assays were run in triplicates and the data are averages of three biological replicates.

Mouse Serum and Flt3 ELISA

Mice were humanely euthanized on day 0, 1, 4, 7, 15 and 30 after TBI (4 and 8 Gy) for serum and tissue collection. Six mice per group were used: nonirradiated vehicle (Veh 0 Gy); nonirradiated GT3 (GT3 0 Gy); Veh 4 Gy; GT3 4 Gy; Veh 8 Gy; and GT3 8 Gy. The mice were deeply anesthetized prior to whole-blood collection through the inferior vena cava in accordance with the approved IACUC protocol. The animals were deeply anesthetized with isoflurane (Abbott Laboratories, Chicago, IL) in a rodent anesthesia machine; the tail was pinched to check reflexive movement indicative of insufficient anesthesia. If there was no response, the animal was moved to a station with an individual nose cone for continued anesthesia. An incision was made on the right side of the animal, close to the inferior vena cava, the vein was exposed and blood was drawn with a 23G needle. Blood was collected in serum separator tubes and allowed to clot for 30 min at room temperature. After centrifugation at 1,500g for 10 min, serum was transferred to a micro-centrifuge tube and stored at -80°C until use. Following the manufacturer's instructions mouse Flt3L was measured by using the commercially available sandwich ELISAs kits (R&D SystemsTM, Minneapolis, MN).

Pathway Analyses

Gene networks and canonical pathways representing key genes were identified through the use of Ingenuity Pathway Analysis (IPA).

Briefly, the data sets containing gene identifiers and corresponding fold change and *P* values were uploaded into the web-delivered application and each gene identifier was mapped to its corresponding gene object in the IPA software. MicroRNA and mRNA relationship analysis was generated using TargetScan Release 5.1 (Whitehead Institute, Cambridge, MA) for miRNA biological target prediction and IPA.

Statistical Analysis

For microarray analysis, each probe was repeated three times on chips from three biological replicates to ensure reproducibility of microarrays and for statistical consideration. Data were analyzed by first subtracting the background and then normalizing the signals using a LOWESS filter (locally-weighted regression) (31). miRNA expression data between two groups were subjected to *t* test and differentially detected signals (>500) were those with *P* < 0.05. All other data sets are expressed as mean \pm standard error of mean (SEM). All experiments were performed independently at least twice and biological replicates were used for each data set. GraphPad Prism v. 6.07 for windows was used for data analysis. Statistical significance was considered at *P* < 0.05. The differences among days, regimens (vehicle and GT3) and radiation doses (4 and 8 Gy) were analyzed by performing a multiple comparisons test using Tukey's honest significant difference test to find means that are significantly different from each other.

RESULTS

GT3 Modulates the Expression of miRs in Irradiated Mouse Spleen in a Dose- and Time-Dependent Manner

Comprehensive analysis of the expressions of 1,265 mature miRs in irradiated mouse spleen tissue with or without prior GT3 treatment was performed at different time intervals. The expression profile of miRs was analyzed in control (naïve, sham-irradiated vehicle and GT3), irradiated vehicle- and GT3-treated samples. All data presented were compared with sham-irradiated vehicle control groups since no difference in the expression of miRs was observed in the microarray analysis between naïve and vehicle-treated groups. As shown in Fig. 1, the miR expression varies in a dose- and time-dependent manner in response to GT3 treatment. Both exposure to radiation and GT3 pretreatment altered the expression of a large number of miRs in spleen tissue compared to the nonirradiated vehicle-treated group (Fig. 1 and Supplementary Figs. S1 and S2).

The Venn diagram shown in Fig. 2 represents 4 (panel A) and 8 Gy (panel B) TBI, showing significantly altered expression of 146 and 351 miRs, respectively, compared to 160 miRs in nonirradiated spleen samples on day 1. Surprisingly, a highly significant dose-dependent increase in the number of overlapping miRs was observed on day 1. Specifically, 12 and 62 miRs were shared with the nonirradiated vehicle-treated group after 4 and 8 Gy TBI, respectively (Fig. 2A and B). Similarly, radiation exposure resulted in higher expression of miRs in spleen tissue on day 4, and 250 and 239 miRs were differentially modulated after 4 and 8 Gy TBI, respectively, compared to nonirradiated spleen tissue on day 4 (Fig. 2C and D).

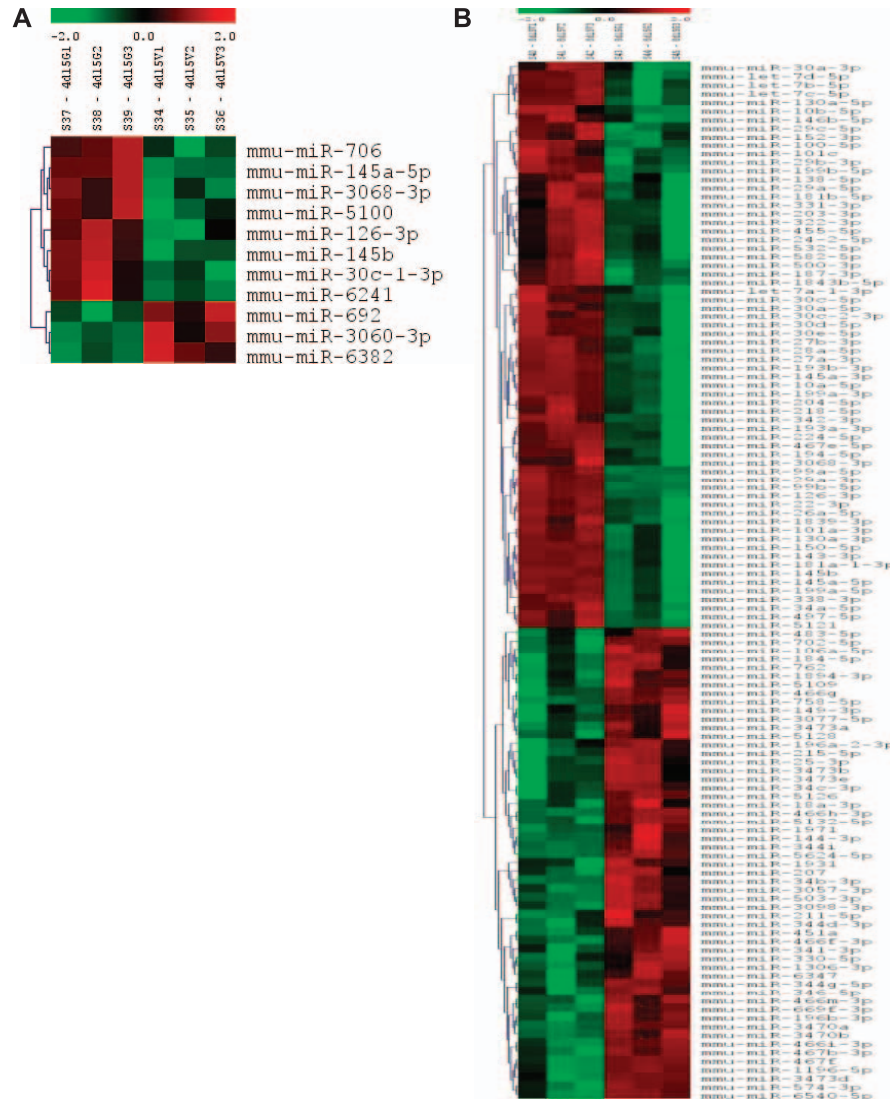


FIG. 1. Identification of differentially expressed spleen miRNAs with varying doses on day 15. CD2F1 mice were exposed to 4 and 8 Gy gamma radiation. The isolated RNA was analyzed by miRNA microarray. The miRNA expression profile in the indicated groups are depicted as 4 Gy Veh vs. 4 Gy GT3 (panel A) and 8 Gy Veh vs. 8 Gy GT3 (panel B) ($n = 3$, $P < 0.05$). The three columns represent three biological replicates from each group. Colors represent log2 values from -2.0 to $+2.0$.

Moreover, miR expression increased in a dose-dependent manner. For example, 50 and 75 miRs were shared with the vehicle-treated sham-irradiated group, respectively, after 4 and 8 Gy irradiation on day 4 (Fig. 2C and D). Additionally, 4 and 8 Gy TBI for 15 days modified the expression of 361 and 329 miRs, respectively. These alterations in miR expression were significantly higher than in the nonirradiated vehicle-treated group (Fig. 2E and F). A similar dose-dependent increase in the number of shared miRs with the nonirradiated vehicle-treated group was observed at day 15, and overlaps of 10 and 31 miRs were found after 4 and 8 Gy TBI, respectively (Fig. 2E and F). GT3 pretreatment altered the expression of 350 against 361 and 369 against 329 miRs after 4 and 8 Gy TBI, respectively, on day 15 (Fig. 2E and F). Moreover, the number of shared miRs between GT3-treated and untreated groups of irradiated mice was

significantly increased in a dose-dependent manner on day 15, and an overlap of 6 and 74 miRs was observed after 4 and 8 Gy, respectively (Fig. 2G and H).

GT3 Suppresses Radiation-Induced Upregulation of miRs

We observed significant upregulation in the expression of a number of miRs associated with hematopoiesis postirradiation on day 1, 4 and 15. However, the magnitude of increase tended to decline by day 15 (Fig. 1). In our previous work, we reported that after a sublethal dose of radiation, maximal suppression of peripheral blood cell count was observed by day 4 with significant recovery by day 15 (8, 9). Thus, in our current work we focused on irradiated spleen tissue with or without GT3 pretreatment harvested on day 15 postirradiation. We also observed that

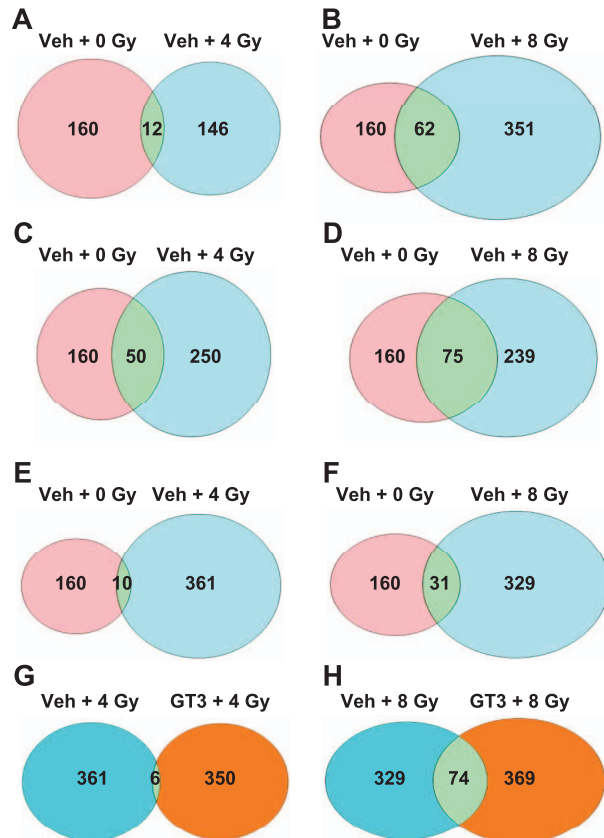


FIG. 2. A Venn diagram of up- and downregulated miRNAs in spleen from mice exposed to 4 and 8 Gy TBI. Degree of overlap is shown at (panel A) day 1 postirradiation between nonirradiated veh and 4 Gy Veh, (panel B) day 1 postirradiation between nonirradiated Veh and 8 Gy Veh, (panel C) day 4 postirradiation between nonirradiated Veh and 4 Gy Veh, (panel D) day 4 postirradiation between nonirradiated Veh and 8 Gy Veh, (panel E) day 15 postirradiation between nonirradiated Veh and 4 Gy Veh, (panel F) day 15 postirradiation between nonirradiated Veh and 8 Gy Veh, (panel G) day 15 postirradiation (4 Gy) between Veh and GT3-treated groups, and (panel H) days postirradiation (8 Gy) between Veh and GT3-treated groups.

the expression of a larger number of miRNAs was altered after 8 Gy compared to that at 4 Gy TBI (data not shown).

Exposure to 8 Gy TBI significantly ($P < 0.05$) upregulated the expression of miR-27b, miR-34a, miR-99b, miR-125b, miR-126, miR-130a, miR-143 and miR-145b compared to the nonirradiated vehicle-treated group on day 15, as detected by microarray analysis (Fig. 3). Interestingly, GT3 pretreatment significantly ($P < 0.05$) suppressed upregulation of these miRNAs on day 15 in 8 Gy irradiated spleen samples (Fig. 3). However, no difference in the expression pattern of miRNAs was observed in sham-irradiated vehicle-treated and sham-irradiated GT3-treated groups, suggesting that GT3 treatment alone does not alter expression of miRNAs (Fig. 3). Further validation of some of the microarray data was performed by qRT-PCR using miR-specific TaqMan assays. These data revealed that the expression of miR-130a and miR-145 was increased about two- and threefold, respectively, after 8 Gy TBI on day 15,

while GT3 pretreatment significantly suppressed the overexpression of these two miRNAs (Supplementary Fig. S3).

GT3 Prevents Postirradiation Downregulation of the Expression of miRNAs in Mouse Spleen Samples

We also observed a downregulation in the expression of miRNAs in spleen samples after TBI, as detected by microarray analysis. The expression of miR-15b and miR-92b significantly ($P < 0.05$) decreased in response to exposure on day 1, but was unaltered up to 4 days (Supplementary Fig. S5). However, the expression of miRNAs was restored at day 15 after 8 Gy TBI (Supplementary Fig. S5). Moreover, GT3 pretreatment promoted postirradiation recovery of miR-15b (Fig. 4). Consistently, Taqman qRT-PCR assay of miR-15b also indicated a significant ($P < 0.05$) postirradiation downregulation, and a GT3-mediated recovery after 15 days of 8 Gy irradiation (Supplementary Fig. S4). We also observed a dose-dependent downregulation of miR-92b on day 4 (data not shown). Wheel diagrams represent the spectrum of the expression of miRNAs, which were substantially altered after irradiation with or without GT3 treatment (Supplementary Fig. S7).

GT3 Suppresses Radiation-Induced p53 mRNA Upregulation

Next, we determined the effect of GT3 on p53 expression after irradiation, because p53 regulates hematopoiesis partly by modulating miR-34a expression. Expression of p53 mRNA increased about 3.5-fold on day 15 after 8 Gy TBI, while GT3 pretreatment significantly ($P = 0.001$) suppressed radiation-induced p53 upregulation in spleen tissue (Fig. 5A). Further network analyses (IPA) indicated TP53 to be associated directly or indirectly with the radiation-responsive aberrantly expressed miRNAs (Fig. 5B).

GT3 Represses Radiation-Induced Flt3L in Mouse Serum

The radiation-induced Flt3L levels increased in a dose- and time-dependent manner (Fig. 6). Baseline levels were 294 (± 46) pg ml⁻¹ and 242 (± 15) pg ml⁻¹, respectively. Flt3L levels were gradually increased after irradiation, and reached maximum levels on day 4 for animals exposed to 4 Gy and day 7 for animals exposed to 8 Gy. There was a significant dose-dependent increase in Flt3 levels from 4 to 8 Gy in vehicle-treated samples on day 1, 4, 7 and 15. On day 7 and 15 at 8 Gy irradiation, Flt3L levels were significantly ($P < 0.01$) inhibited by GT3 pretreatment (Fig. 6). At day 1, Flt3L levels were 480 (± 17) pg ml⁻¹ and 818 (± 77) pg ml⁻¹ for vehicle-treated animals irradiated at 4 and 8 Gy, respectively. At day 4, Flt3L levels were 1,147 (± 43) pg ml⁻¹ and 2,196 (± 135) pg ml⁻¹ for vehicle-treated animals irradiated at 4 and 8 Gy, respectively. At day 7, Flt3L levels were 553 (± 53) pg ml⁻¹ and 2,454 (± 103) pg ml⁻¹ for vehicle-treated animals irradiated at 4 and 8 Gy, respectively.

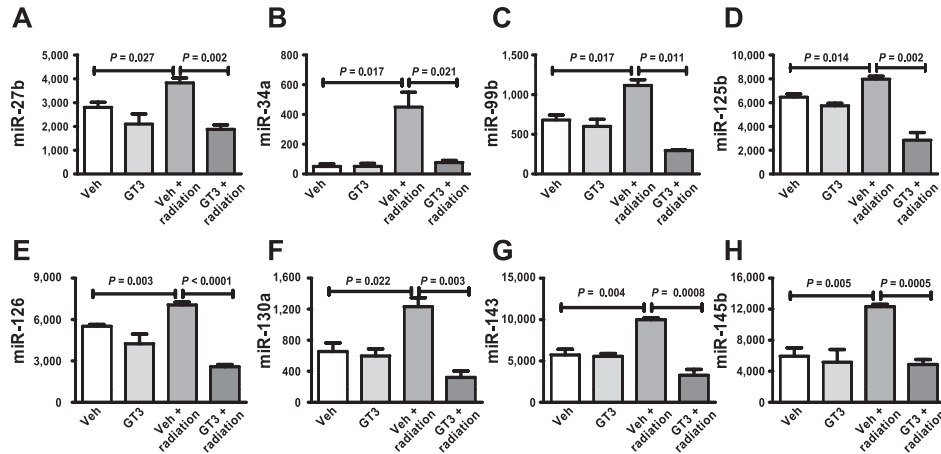


FIG. 3. Radiation-induced upregulation of miRNA expression, inhibited by GT3. CD2F1 mice were 8 Gy TBI and spleens harvested at day 15 postirradiation. Total RNA was extracted from spleens using miRvana RNA isolation kit following manufacturer's protocol. RNA was quantified and its integrity was checked by identifying 28S and 18S bands on agarose gel. Radiation-induced upregulation of (panel A) miR-27b, (panel B) miR-34a, (panel C) miR-99b, (panel D) miR-125b, (panel E) miR-126-3p, (panel F) miR-130a, (panel G) miR-143 and (panel H) miR-145b expressions were blocked by GT3 treatment. All data were collected from three biological replicates and presented as mean \pm standard error of mean.

GT3 Modulates ERK, MAPK and Insulin Pathways in Irradiated Mouse Spleen

We further performed *in silico* analyses of the 1,265 differentially expressed miRNAs using IPA. Networks generated indicated the roles of signaling pathways including ERK, MAPK and insulin pathways as key players in radiation-induced hematopoiesis (Fig. 7). IPA-generated diseases and molecular functions indicated that radiation exposure and/or GT3 highly influence hematopoietic cancers, such as chronic B-cell leukemia (Fig. 8), lymphocytic leukemia (Fig. 9) and lymphohematopoietic cancer (Fig. 10). These data clearly indicated that GT3 plays a critical role in radiation-induced hematopoiesis, under normal as well as disease conditions, by modulating miR-mediated signal transduction pathways. In addition, the effect of radiation exposure and/or GT3 in various diseases and cellular functions is summarized in Supplementary Fig. S8.

DISCUSSION

In this study, GT3 pretreatment significantly enhanced survival in mice that received lethal TBI. GT3 accelerates blood cell recovery in mice that received sublethal TBI on day 15 (8), as well as protected hematopoietic stem and progenitor cells, and helped in regeneration of sternal bone marrow cellularity after 7 Gy TBI by day 14 (9). Moreover, GT3 enhances the number of spleen colony-forming units as well as spleen size in CD2F1 mice after 8.5 Gy TBI by day 12 (10) compared to vehicle-treated irradiated groups. Since we previously reported that radiation exposure causes maximal suppression of peripheral blood cell count by day 4 with significant recovery by day 15 after sublethal irradiation, our current study focused on irradiated spleen

tissue with or without GT3 pretreatment harvested 15 days after TBI (8, 9). Flt3L can be regarded as a radiation-specific biomarker of radiation-induced aplasia (28). Our data shows that there is a dose- (4 and 8 Gy) and time- (day 0–15) dependent increase in serum levels of Flt3L, after TBI, and there is a significant inhibition of serum levels of Flt3L in GT3-treated animals. These data clearly indicate that at day 15 (8 Gy), there was a pronounced effect by GT3 in protecting the animals from hematopoietic death.

The important role of miRs in the regulation of radiation-induced injury has emerged from several recent studies.

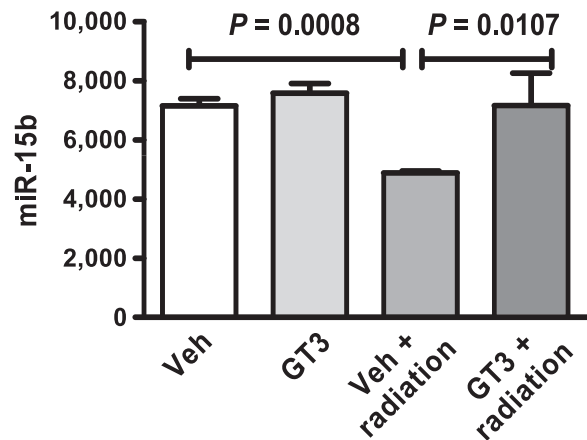


FIG. 4. GT3 attenuated radiation-induced downregulation of miR-15b expression. CD2F1 mice were whole-body irradiated with 8 Gy and spleens harvested at 15 days postirradiation. Total RNA was extracted from spleen using miRvana RNA isolation kit following manufacturer's protocol. RNA was quantified and its integrity was checked by identifying 28S and 18S bands on agarose gel. Expression of miR-15b was significantly suppressed in the spleen sample as a result of radiation, while GT3 pretreatment returned it to normal. All data were collected from three biological replicates and presented as mean \pm standard error of mean.

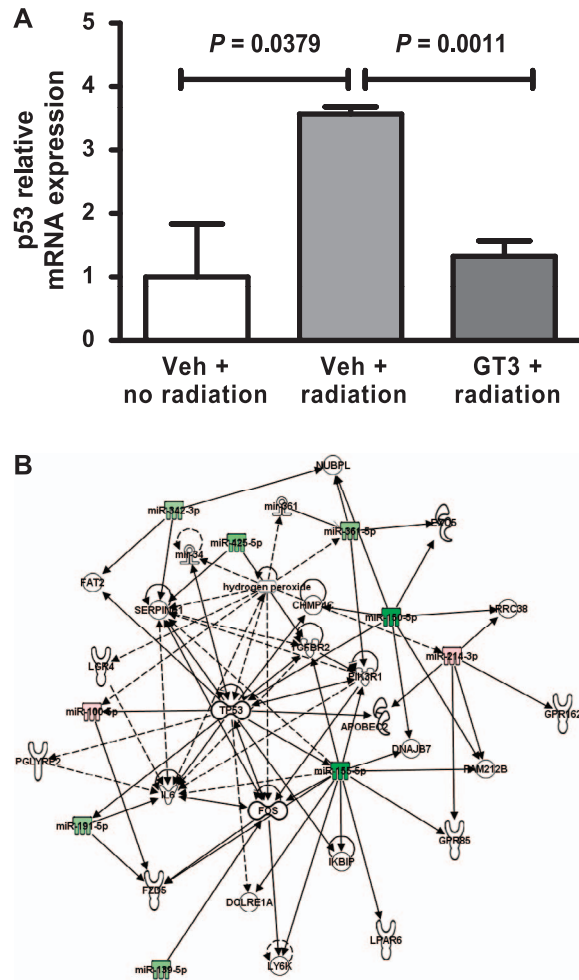


FIG. 5. Regulation of p53, a miR-34a target, by GT3. Panel A: p53 miRNA expression was determined by qRT-PCR in spleens from CD2F1 mice on day 15 postirradiation from nonirradiated vehicle (Veh + NIR), 8 Gy vehicle (Veh + IR) and 8 Gy GT3 (GT3 + IR). p53 was induced after irradiation and was suppressed by GT3 treatment. The data ($P < 0.05$) reflects the average of three or more independent experiments and are shown as mean \pm standard error of mean. Panel B: IPA analyses of the miR-associated pathways in controls compared to radiation exposure (8 Gy GT3 15 days) also indicates a TP53 focused network (green: downregulated and red: upregulated).

Radiation-induced miRs in plasma or serum can be predictive biomarkers for dosimetry to assess dose after mass casualty incidents and it may provide a valuable tool in developing and implementing radiation countermeasures. Radiation-induced miRs may also play significant roles in targeting signaling pathways. In this study, we identify the radiation-induced miRs that are modulated by GT3 in the hematopoietic spleen tissue of mice. We report here for the first time that GT3 modulates the expression of miRs in irradiated mouse spleen in a dose- and time-dependent manner.

Gaedicke *et al.* reported that the difference in dietary vitamin E differentially modulates expressions of hepatic miRs in rats including miR-125b, which is known to play a critical role in regulating normal hematopoiesis at the stem

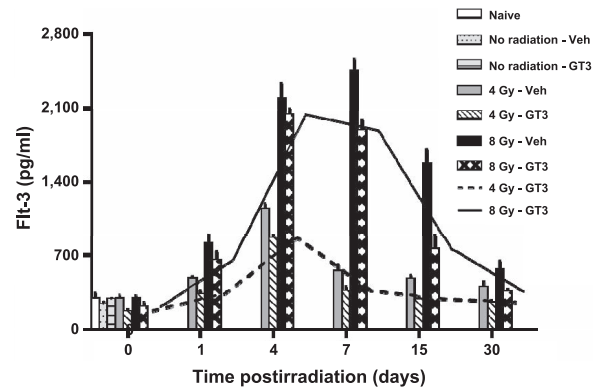
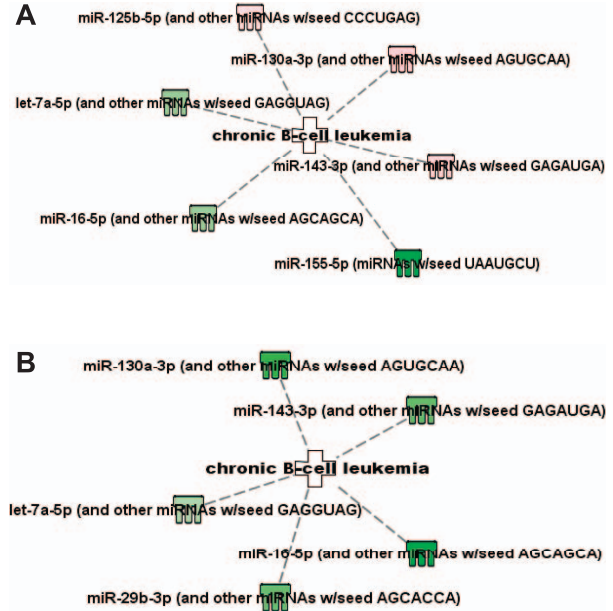


FIG. 6. Dose- and time-dependent changes for Flt3L and modulation by GT3. CD2F1 mice were 4 and 8 Gy TBI and blood was harvested on day 1, 4, 7, 15 and 30 postirradiation for serum separation. Flt3L expression was analyzed by ELISA. A dose- and time-dependent increase in Flt3L was observed up to day 7. Flt3L levels were significantly inhibited by pretreatment with GT3 on day 7 and 15 ($P < 0.05$). The data reflects the average of three or more independent experiments and are presented as mean \pm standard error of mean.

cell level. The overexpression of miR-125b results in hematopoietic malignancies, such as acute myeloid leukemia, acute lymphoblastic leukemia and multiple myeloma (13). Moreover, a recent study demonstrated that miR-125b regulates human bone marrow precursor B-cell differentiation (32). These data suggest that miR-125b, which is modulated by vitamin E, may play a critical role in normal hematopoiesis as well as in hematopoietic malignancy. Here, we determined the effect of GT3 in regulating the expression pattern of miRs in irradiated spleen tissue to gain better insight on the role of miRs in GT3-mediated postirradiation hematopoietic recovery.

Our study reveals that an array of miRs, which directly or indirectly influence normal, as well as abnormal hematopoiesis, is overexpressed in spleen tissue of irradiated mice and are substantially suppressed by GT3 pretreatment. We noticed that miR-125b, which is involved in hematopoiesis and lymphomagenesis, is significantly ($P = 0.014$) overexpressed in irradiated spleen tissue, and GT3 pretreatment suppressed its upregulation. Earlier studies have demonstrated the role of miR-125b in myeloid and lymphoid malignancies (33, 34). Moreover, it has also been shown that overexpression of miR-125b is associated with enhanced tumor growth and a shorter median survival in a cutaneous T-cell lymphoma (CTCL) model (35). Therefore, based on our data we hypothesize that GT3-mediated suppression of radiation-induced miR-125b upregulation may prevent hematopoietic malignant transformation and protect the hematopoietic spleen tissue.

A number of studies have established the role of miRs in the pathogenesis of various types of cancer. Genetic screening has identified miR cluster 99b/let-7e/125a as a critical regulator of hematopoietic stem/progenitor cell differentiation. The overexpression of this cluster leads to an increased myeloid differentiation, and subsequent



Next, we determined the consequence of GT3 pretreatment on the expression of tumor suppressor p53 after irradiation. The expression of p53 is altered after irradiation (40) and has been shown to regulate hematopoiesis (41). Additionally, p53 modulates the expression of a substantial number of miRs, particularly in response to DNA damage (42), for example, p53 is one of the strongest inducers of miR-34a after DNA damage (43). Another study showed

development of myeloproliferative neoplasms in mice (36). Gain-of-function analysis has demonstrated that constitutive expression of miR-34a blocks B-cell development by inhibiting transcription factor Foxp1, finally resulting in reduction in mature B cells in mice (37). A recent screening of AML patient samples has illustrated that miR-130a is significantly upregulated (25) in AML patients, while

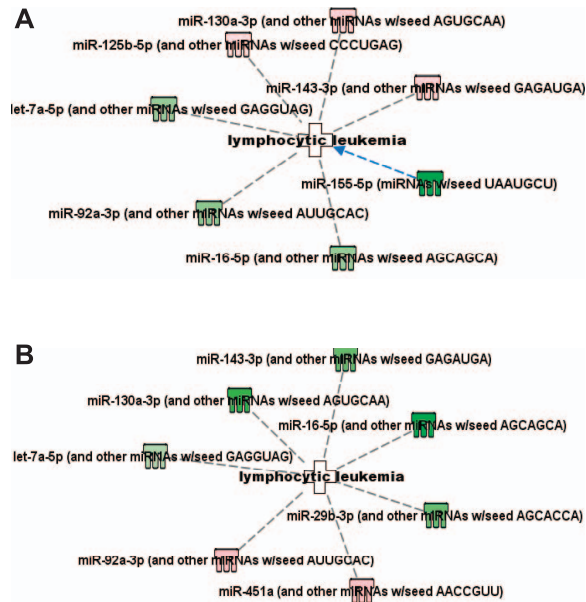


FIG. 9. Radiation-responsive miRNAs are linked to lymphocytic leukemia. The analyses of all the miRs that exhibit significant changes in expression in the nonirradiated Veh, 8 Gy day 15 Veh, and 8 Gy day 15 GT3 indicate lymphocytic leukemia as a focus. Panel A: Nonirradiated Veh vs. 8 Gy day 15 Veh. Panel B: 8 Gy day 15 Veh vs. 8 Gy day 15 GT3. (Green indicates downregulated; red indicates upregulated)

that exposure to radiation caused upregulation of p53 in mucosa of patients undergoing radiotherapy (40). Additionally, increased expression of wild-type p53 was observed in lymphocytes of patients with chronic lymphatic leukemia (44). Consistently, we also observed a significant ($P = 0.0379$) increase in p53 expression in irradiated mouse spleen. Moreover, we observed increased expression of miR-34a postirradiation, as expected, possibly inducing the upregulation of its target gene p53 (18, 43). GT3 pretreatment attenuates radiation-induced p53 as well as miR-34a overexpression, suggesting its possible role in protecting the spleen from radiation-induced damage by day 15 after a sublethal dose of TBI.

In concurrence with the observation by Jacob *et al.* (16), we observed a dose-dependent decrease in spleen miR-150 expression after irradiation (Supplementary Fig. S6). There was a significant decrease in miR-150 expression by day 1 postirradiation, which remained unchanged up to day 15 after TBI. Dose-dependent decrease in miR-150 was observed at all exposure time intervals analyzed (Supplementary Fig. S6). Li *et al.* (17) reported that miR-30b and miR-30c were upregulated by radiation exposure in the human hematopoietic cells by 1 h after gamma irradiation. In contrast, we did not observe upregulation of miR-30 family in (mouse) spleen postirradiation at any time points. We recently reported that DT3 completely blocked the expression of miR-30 families in bone marrow, jejunum and liver within 1 h postirradiation, whereas in serum, the effect was found up to 24 h postirradiation. In that study, we did not observe any effect of GT3 on miR-30 expression in

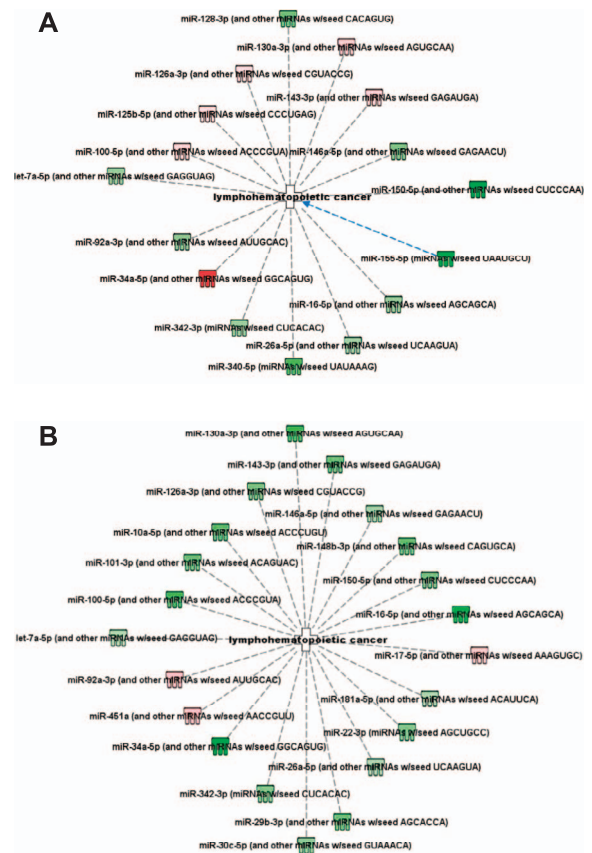


FIG. 10. Radiation-responsive miRNAs are linked to lymphohematopoietic cancer. Analyses of all the miRs that exhibit significant changes in expression in the nonirradiated Veh, 8 Gy day 15 Veh and 8 Gy day 15 GT3 indicate lymphohematopoietic cancer as a major focus. Panel A: Nonirradiated Veh vs. 8 Gy day 15 Veh. Panel B: 8 Gy day 15 Veh vs. 8 Gy day 15 GT3. (Green indicates downregulated; red indicates upregulated).

spleen at early (24 h) or later time points (day 4 and 15) after irradiation (27), suggesting that radiation-induced miR-30 could be tissue specific. However, analyzing miRNA status at earlier times (even before day 1 after irradiation) will be informative (27).

A comprehensive bioinformatics analysis using the IPA program performed with miR expression profile data, as well as the corresponding predicted mRNA targets, indicate that cellular signaling pathways including ERK, MAPK and insulin pathways are the key targets in GT3-treated irradiated spleen samples. These pathways have been known to be involved in hematopoiesis and lymphomagenesis (45–50). These data indicate that postirradiation hematopoietic protection by GT3 might be regulated through the ERK/P38-MAPK signaling pathway. Consistently, networks generated by IPA indicate that these radiation-responsive miRs are associated with hematopoietic cancer-related development, with hubs focusing on lymphohematopoietic cancer. Furthermore, treatment with GT3 reversed the differential regulation of miR-34a, miR-92b, miR-125b, miR-130a and miR-143-3p that are associated with leukemogenesis. These data clearly suggest

that GT3 pretreatment plays a significant role in suppressing radiation-induced hematopoietic malignancy as well as hematopoietic injury. Functional analysis and characterization of the associated molecules are part of our future goals.

In conclusion, our studies with irradiated mouse spleen tissue show that GT3 pretreatment reverses the expression of several miRs, which are involved in postirradiation hematopoiesis. *In silico* cellular pathway analyses implicate ERK/P38MAPK as target signaling pathways for the recovery of radiation-induced damage in spleen by GT3. The role of radiation-responsive miRs in the regulation of these signaling pathways warrants further studies.

SUPPLEMENTARY MATERIALS

Supplementary materials are available online at: <http://dx.doi.org/10.1667/RR14248.1.S1>.

ACKNOWLEDGMENTS

This study was supported by the U.S. Department of Defense Threat Reduction Agency (grant no. H.10016_09_AR_R), administered by The Henry M. Jackson Foundation for the Advancement of Military Medicine, Inc. and the National Institute of General Medical Sciences (NIGMS grant no. P20 GM109005) from the National Institutes of Health. The authors have no conflict of interest, financial or otherwise, to declare. The opinions contained herein are the private views of the authors and are not necessarily those of the Armed Forces Radiobiology Research Institute, the Uniformed Services of the University of the Health Sciences or the Department of Defense.

Received: August 26, 2015; accepted: February 20, 2016; published online: April 29, 2016

REFERENCES

1. Baskar R, Lee KA, Yeo R, Yeoh KW. Cancer and radiation therapy: current advances and future directions. *Int J Med Sci* 2012; 9:193–9.
2. Bentzen SM. Preventing or reducing late side effects of radiation therapy: radiobiology meets molecular pathology. *Nat Rev Cancer* 2006; 6:702–13.
3. Hauer-Jensen M, Kumar KS, Wang J, Berbee M, Fu Q, Boerma M. Intestinal toxicity in radiation and combined injury: significance, mechanisms, and countermeasures. Larche R, editor. Hauppauge, NY: NOVA Science Publishers Inc; 2008.
4. Hendry JH, Feng-Tong Y. Response of bone marrow to low LET irradiation. In: Hendry JH, Lord BI, editors. *Radiation toxicology: bone marrow and leukemia*. London: Taylor & Francis; 1995. p. 91–116.
5. Fliedner TM, Nothdurft W, Heit H. Biological factors affecting the occurrence of radiation syndromes. In: Broerse JJ, MacVittie TJ, editors. *Response of different species to total body irradiation*. Martinus Nijhoff Publishers; 1984. p. 209–19.
6. Mauch P, Constine L, Greenberger J, Knospe W, Sullivan J, Liesveld JL, et al. Hematopoietic stem cell compartment: acute and late effects of radiation therapy and chemotherapy. *Int J Radiat Oncol Biol Phys* 1995; 31:1319–39.
7. Committee on Health. Risk of ionizing radiation exposure to children: a subject review. American Academy of Pediatrics. Committee on Environmental Health. *Pediatrics* 1998; 101(4 Pt 1): 717–9.
8. Ghosh SP, Kulkarni S, Hieber K, Toles R, Romanyukha L, Kao TC, et al. Gamma-tocotrienol, a tocol antioxidant as a potent radioprotector. *Int J Radiat Biol* 2009; 85:598–606.
9. Kulkarni S, Ghosh SP, Satyamitra M, Mog S, Hieber K, Romanyukha L, et al. Gamma-tocotrienol protects hematopoietic stem and progenitor cells in mice after total-body irradiation. *Radiat Res* 2010; 173:738–47.
10. Berbee M, Fu Q, Boerma M, Wang J, Kumar KS, Hauer-Jensen M. gamma-Tocotrienol ameliorates intestinal radiation injury and reduces vascular oxidative stress after total-body irradiation by an HMG-CoA reductase-dependent mechanism. *Radiat Res* 2009; 171:596–605.
11. Shah SJ, Sylvester PW. Gamma-tocotrienol inhibits neoplastic mammary epithelial cell proliferation by decreasing Akt and nuclear factor kappaB activity. *Exp Biol Med* 2005; 230:235–41.
12. Yap WN, Chang PN, Han HY, Lee DT, Ling MT, Wong YC, et al. Gamma-tocotrienol suppresses prostate cancer cell proliferation and invasion through multiple-signalling pathways. *Br J Cancer* 2008; 99:1832–41.
13. Gaedicke S, Zhang X, Schmelzer C, Lou Y, Doering F, Frank J, et al. Vitamin E dependent microRNA regulation in rat liver. *FEBS Lett* 2008; 582:3542–6.
14. Khée SG, Yusof YA, Makpol S. Expression of senescence-associated microRNAs and target genes in cellular aging and modulation by tocotrienol-rich fraction. *Oxid Med Cell Longev* 2014; 2014:725929.
15. Acharya SS, Fendler W, Watson J, Hamilton A, Pan Y, Gaudiano E, et al. Serum microRNAs are early indicators of survival after radiation-induced hematopoietic injury. *Sci Transl Med* 2015; 7:287ra69.
16. Jacob NK, Cooley JV, Yee TN, Jacob J, Alder H, Wickramasinghe P, et al. Identification of sensitive serum microRNA biomarkers for radiation biodosimetry. *PloS One* 2013; 8:e57603.
17. Li XH, Ha CT, Fu D, Xiao M. Micro-RNA30c negatively regulates REDD1 expression in human hematopoietic and osteoblast cells after gamma-irradiation. *PloS One* 2012; 7:e48700.
18. Liu C, Zhou C, Gao F, Cai S, Zhang C, Zhao L, et al. MiR-34a in age and tissue related radio-sensitivity and serum miR-34a as a novel indicator of radiation injury. *Int J Biol Sci* 2011; 7:221–33.
19. Simone NL, Soule BP, Ly D, Saleh AD, Savage JE, Degraff W, et al. Ionizing radiation-induced oxidative stress alters miRNA expression. *PloS One* 2009; 4:e6377.
20. Cui W, Ma J, Wang Y, Biswal S. Plasma miRNA as biomarkers for assessment of total-body radiation exposure dosimetry. *PloS One* 2011; 6:e22988.
21. Ishii H, Saito T. Radiation-induced response of micro RNA expression in murine embryonic stem cells. *Med Chem* 2006; 2:555–63.
22. Josson S, Sung SY, Lao K, Chung LW, Johnstone PA. Radiation modulation of microRNA in prostate cancer cell lines. *Prostate* 2008; 68:1599–606.
23. Wagner-Ecker M, Schwager C, Wirkner U, Abdollahi A, Huber PE. MicroRNA expression after ionizing radiation in human endothelial cells. *Radiat Oncol* 2010; 5:25.
24. Illytskyy Y, Zemp FJ, Koturbash I, Kovalchuk O. Altered microRNA expression patterns in irradiated hematopoietic tissues suggest a sex-specific protective mechanism. *Biochem Biophys Res Commun* 2008; 377:41–5.
25. Li Z, Lu J, Sun M, Mi S, Zhang H, Luo RT, et al. Distinct microRNA expression profiles in acute myeloid leukemia with common translocations. *Proc Natl Acad Sci U S A* 2008; 105:15535–40.
26. Lazare SS, Wojtowicz EE, Bystrykh LV, de Haan G. microRNAs in hematopoiesis. *Exp Cell Res* 2014; 329:234–8.
27. Li XH, Ha CT, Fu D, Landauer MR, Ghosh SP, Xiao M. Delta-tocotrienol suppresses radiation-induced microRNA-30 and protects mice and human CD34+ cells from radiation injury. *PloS One* 2015; 10:e0122258.

28. Ossetrova NI, Condliffe DP, Ney PH, Krasnopolsky K, Hieber KP, Rahman A, et al. Early-response biomarkers for assessment of radiation exposure in a mouse total-body irradiation model. *Health Phys* 2014; 106:772–86.
29. Gao X, Gulari E, Zhou X. In situ synthesis of oligonucleotide microarrays. *Biopolymers* 2004; 73:579–96.
30. Zhu Q, Hong A, Sheng N, Zhang X, Matejko A, Jun KY, et al. microParaflo biochip for nucleic acid and protein analysis. *Methods Mol Biol* 2007; 382:287–312.
31. Bolstad BM, Irizarry RA, Astrand M, Speed TP. A comparison of normalization methods for high density oligonucleotide array data based on variance and bias. *Bioinformatics* 2003; 19:185–93.
32. Jensen K, Brusletto BS, Aass HC, Olstad OK, Kierulf P, Gautvik KM. Transcriptional profiling of mRNAs and microRNAs in human bone marrow precursor B cells identifies subset- and age-specific variations. *Plos One* 2013; 8:e70721.
33. Bousquet M, Quelen C, Rosati R, Mansat-De Mas V, La Starza R, Bastard C, et al. Myeloid cell differentiation arrest by miR-125b-1 in myelodysplastic syndrome and acute myeloid leukemia with the t(2;11)(p21;q23) translocation. *J Exp Med* 2008; 205:2499–506.
34. Sonoki T, Iwanaga E, Mitsuya H, Asou N. Insertion of microRNA-125b-1, a human homologue of lin-4, into a rearranged immunoglobulin heavy chain gene locus in a patient with precursor B-cell acute lymphoblastic leukemia. *Leukemia* 2005; 19:2009–10.
35. Manfe V, Biskup E, Willumsgaard A, Skov AG, Palmieri D, Gasparini P, et al. cMyc/miR-125b-5p signalling determines sensitivity to bortezomib in preclinical model of cutaneous T-cell lymphomas. *Plos One* 2013; 8:e59390.
36. Gerrits A, Walasek MA, Olthof S, Weersing E, Ritsema M, Zwart E, et al. Genetic screen identifies microRNA cluster 99b/let-7e/125a as a regulator of primitive hematopoietic cells. *Blood* 2012; 119:377–87.
37. Rao DS, O'Connell RM, Chaudhuri AA, Garcia-Flores Y, Geiger TL, Baltimore D. MicroRNA-34a perturbs B lymphocyte development by repressing the forkhead box transcription factor Foxp1. *Immunity* 2010; 33:48–59.
38. Hager M, Pedersen CC, Larsen MT, Andersen MK, Hother C, Gronbaek K, et al. MicroRNA-130a-mediated down-regulation of Smad4 contributes to reduced sensitivity to TGF-beta1 stimulation in granulocytic precursors. *Blood* 2011; 118:6649–59.
39. Sengupta S, Nie J, Wagner RJ, Yang C, Stewart R, Thomson JA. MicroRNA 92b controls the G1/S checkpoint gene p57 in human embryonic stem cells. *Stem Cells* 2009; 27:1524–8.
40. Marijnen CA, Kapiteijn E, Nagtegaal ID, Mulder-Stapel AA, van de Velde CJ, Schrier PI, et al. p53 expression in human rectal tissue after radiotherapy: upregulation in normal mucosa versus functional loss in rectal carcinomas. *Int J Radiat Oncol Biol Phys* 2002; 52:720–8.
41. Pant V, Quintas-Cardama A, Lozano G. The p53 pathway in hematopoiesis: lessons from mouse models, implications for humans. *Blood* 2012; 120:5118–27.
42. Hattori H, Janky R, Nietfeld W, Aerts S, Madan Babu M, Venkitaraman AR. p53 shapes genome-wide and cell type-specific changes in microRNA expression during the human DNA damage response. *Cell Cycle* 2014; 13:2572–86.
43. Chang TC, Wentzel EA, Kent OA, Ramachandran K, Mullendore M, Lee KH, et al. Transactivation of miR-34a by p53 broadly influences gene expression and promotes apoptosis. *Mol Cell* 2007; 26:745–52.
44. Peller S. Clinical implications of p53: effect on prognosis, tumor progression and chemotherapy response. *Semin Cancer Biol* 1998; 8:379–87.
45. Huang HL, Hsieh MJ, Chien MH, Chen HY, Yang SF, Hsiao PC. Glabridin mediate caspases activation and induces apoptosis through JNK1/2 and p38 MAPK pathway in human promyelocytic leukemia cells. *Plos One* 2014; 9:e98943.
46. Kale VP. Differential activation of MAPK signaling pathways by TGF-beta1 forms the molecular mechanism behind its dose-dependent bidirectional effects on hematopoiesis. *Stem Cells Dev* 2004; 13:27–38.
47. Landreth KS, Narayanan R, Dorshkind K. Insulin-like growth factor-I regulates pro-B cell differentiation. *Blood* 1992; 80:1207–12.
48. Stein R, Gupta P, Chen X, Cardillo TM, Furman RR, Chen S, et al. Therapy of B-cell malignancies by anti-HLA-DR humanized monoclonal antibody, IMMU-114, is mediated through hyperactivation of ERK and JNK MAP kinase signaling pathways. *Blood* 2010; 115:5180–90.
49. Zhang C, Lv J, He Q, Wang S, Gao Y, Meng A, et al. Inhibition of endothelial ERK signalling by Smad1/5 is essential for haematopoietic stem cell emergence. *Nat Commun* 2014; 5:3431.
50. Zumkeller W. The insulin-like growth factor system in hematopoietic cells. *Leuk Lymphoma* 2002; 43:487–91.